

Rigorous Design of a Switched Reluctance Motor Using a Hybrid Design Model

Zwe-Lee Gaing*, Yao-Yang Hsieh*, Mi-Ching Tsai**
Min-Fu Hsieh** and Ming-Hsiao Tsai**

Abstract— Torque ripple is a very essential index for evaluating the effectiveness of a switched reluctance motor (SRM). Many common design strategies for reducing torque ripples of a SRM are changing the excitation trigger angle of stator windings, delaying the cut-off time of winding excitation, adjusting the ratio of arc angle between stator and rotor, and changing the geometric shape of rotor. However, the output torque or the efficiency of the SRM may drop as the above design strategies are solely adopted. In this paper, a hybrid design model which is obtained by the Taguchi Method for optimally designing a SRM with lower torque ripple and higher efficiency is presented. A 12S/8P motor is taken as a study case, and the 3D finite element method (FEM) is applied to analyze the characteristics of the motor and optimize the design process. The results have shown that the proposed method can achieve the design goal of obtaining a high-performance SRM for light electric vehicle applications.

Keyword: Switched reluctance motor, Torque ripple, Taguchi method, Finite element method

1. Introduction

Facing the high price and unstable supplement of rare earth elements, switched reluctance motors (SRMs) are very suitable for adoption as the power motor of electric vehicles (EV). The characteristics of the magnet-less rotor and concentrated winding stator feature SRMs with a simple structure, low production cost, solid structure capable of withstanding harsh environments, higher efficiency and inertia ratio of torque and rotation, simple converter structure, flexible operation capacity and high fault tolerance, and safety and reliability[1]-[4]. Figure 1 shows the structure of a 12S8P (12/8) SRM and the driving circuit.

Because of the geometric shape with double salient poles, when rotating, the traditional SRM produces torque ripples and further causes vibrations and noises. Hence, reducing torque ripples has become the focus in research on developing high efficient SRMs. Referring to [5]-[9], two common design models for effectively reducing torque ripples of a SRM are changing the driver control mode to

make the input current of the SRM more continuous, and changing the geometric shape of the rotor and stator. To elaborate further on the former, altering the driver control mode means modifying the excitation trigger angle of stator windings and delaying the cut-off time of winding excitation. The latter can be simply restated as adjusting the ratio of the arc angle between the stator and rotor and changing the geometric shape of the rotor [6]-[7].

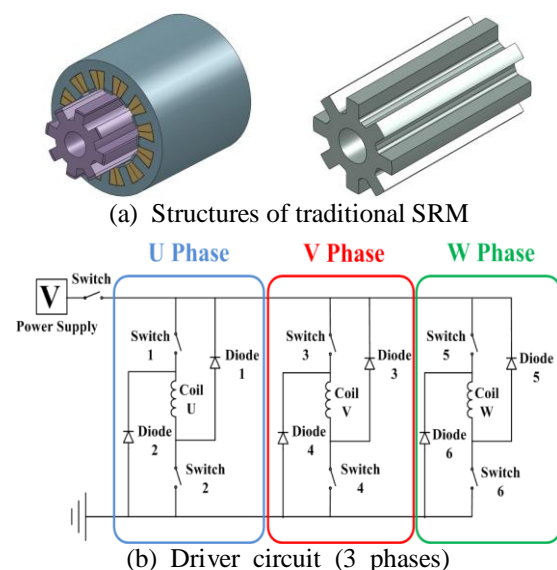


Fig. 1. 3-phase 12/8 SRM

* Dept. of Electrical Engineering, Kao Yuan University, Kaohsiung city 821, Taiwan. (zlgain@cc.kyu.edu.tw)

** Emotors Technology Research Center, National Cheng Kung University, Tainan city 701, Taiwan (ming_hsiao2005@yahoo.com.tw)

However, as the mentioned design strategies are solely adopted, the output torque and the efficiency of the SRM will drop [7]-[11]. Therefore, how to skillfully adopt the mentioned strategies to reach the goal of reducing torque ripple of SRM under the constraints of not lowering the output torque and efficiency, has been widely studied [10]-[18].

In order to achieve the stated research target with low torque ripple and high efficiency, this paper presents a hybrid design model based on four reducing torque ripple strategies: (i) changing the excitation trigger angle of stator windings, (ii) delaying the cut-off time of winding excitation, (iii) adjusting the ratio of arc angle between stator and rotor, and (iv) changing the geometric shapes of rotor. Furthermore, the Taguchi Method is applied to compute the best combination from the above four strategies; thus, the hybrid design strategy model is generated, which is used to optimize the SRM while maintaining the quality criteria of low torque ripple and high efficiency. The process of computation is shown as Fig. 2 [18][19]. A commercially available electrical vehicle SRM of the specification 48V, 12S/8P, rated speed 2400rpm, and rated torque 7.0N-m, is adopted as the study case shown as Fig. 1, and 3D FEM is applied for the simulation and verification.

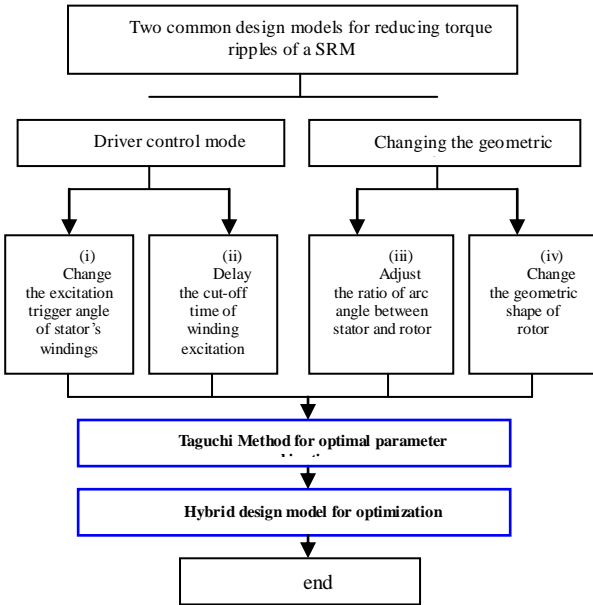


Fig. 2. Proposed design process

2. Mathematical Model of Reluctance Machine

2.1 Torque Equation of Reluctance Machine

The magnetic lines of a magnetic circuit stretch out along the path of least reluctance and form a closed loop. Hence, if the magnetic sheets of the stator and rotor are not in parallel, they will be influenced by the magnetic field effect and shift towards the magnetic path of least reluctance, thus producing a distracting force, i.e., reluctance force. Reluctance motors use such reluctance force to induce the rotation of the rotor to generate torque.

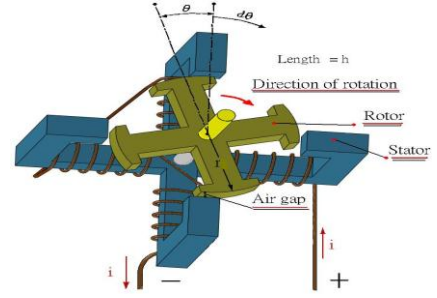


Fig. 3. Simplified structure of a 4-pole reluctance machine.

Fig. 3 shows a simplified structure of a 4-pole reluctance machine. Let the structure be a linear system, via electromechanical energy conversion, and the coenergy W_f' of the system is

$$W_f' = \frac{1}{2} L(\theta) \cdot i^2, \quad (1)$$

with a torque T_f of

$$T_f = \frac{\partial W_f'}{\partial \theta} = \frac{1}{2} i^2 \frac{\partial L(\theta)}{\partial \theta} \quad (2)$$

According to the symmetry characteristics of the magnetic circuit, the inductance generated in a pole-pair can be expressed as [18]

$$L(\theta) = \frac{N^2}{\mathfrak{R}(\theta)} = \frac{N^2 \mu_o (r + 0.5g)\theta}{2g} \quad (3)$$

where the reluctance \mathfrak{R} is a function of θ . Hence, the coenergy W_f' of the 4-pole reluctance machine is [10]

$$W_f' = 2 \cdot \mu_o g H_{ag}^2 h (r + 0.5g) \theta \quad (4)$$

According to (1) and (2), the torque T_f generated by the system can be derived as

$$\begin{aligned} T_f &= \frac{\partial W_f'}{\partial \theta} = 2 \cdot \mu_o g H_{ag}^2 h (r + 0.5g) \\ &= \frac{2 \cdot g B_{ag}^2 h (r + 0.5g)}{\mu_o} \end{aligned} \quad (5)$$

By (5), the reluctance machine takes advantages of the double salient poles structure and unaligned arc angles of the stator and rotor, i.e., $\theta \neq 0$; thus, the reluctance force and torque are produced. However, the torque T_f of the reluctance machine is related to structural geometric factors, such as machine length h , air gap width g , rotor radius r , air-gap flux density B_{ag} , etc.

2.2 Torque Ripple

Torque ripple is produced due to the alignment effect of the magnetic pole teeth of the motor stator and rotor, and the discontinuous input current occurred when switching the driver thyristor [5]-[9]. Figure 4 presents the waveform of reluctance motor torque. The ripple causes the vibrations and noises to motors, which are very essential shortcoming of SRM applications. Hence, the design techniques of reducing torque ripples are widely studied.

Referring to Fig. 4, in order to measure torque ripples, in this paper, the factor of torque ripples is defined as

$$T_{ripple} = \frac{T_{max} - T_{min}}{T_{max}} \times 100\% \tag{6}$$

where T_{ripple} denotes to the factor of torque ripples, and T_{max} and T_{min} represent to the maximal and minimal values of torque, respectively..

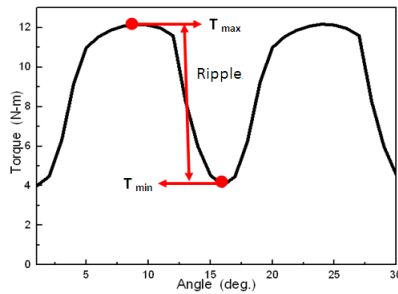


Fig. 4. Torque ripples

By (6), the efficient strategy for reducing torque ripples without affecting average output torque is capable of lowering T_{max} while maximizing T_{min} .

3. Effectiveness Evaluation of Different Design Strategies

Referring to [5]-[17], when the design strategies are applied to reduce torque ripples, output torque of SRM will drop accordingly. Therefore, in this paper, the impact of each strategy to the output properties of the motor, such as torque ripples, output torque, efficiency, etc., are studied

and evaluated in great detail, thus determining the best strategy for reducing torque ripples.

3.1 Change the Excitation Trigger Angle of Stator Windings

The original excitation trigger angle of the 12/8 reluctance motor is 15 degrees, as shown in Fig. 5. In this paper, the early excitation is proposed as in Fig. 6(a), in which the blue dotted line shows the original 0-degree excitation, and the red line displays the 3-degree early excitation.

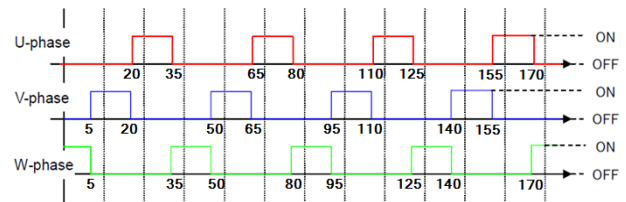
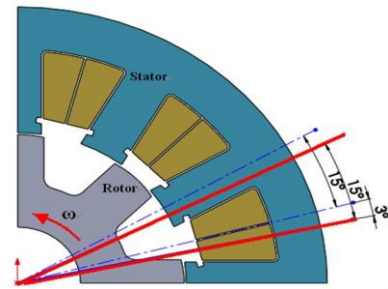
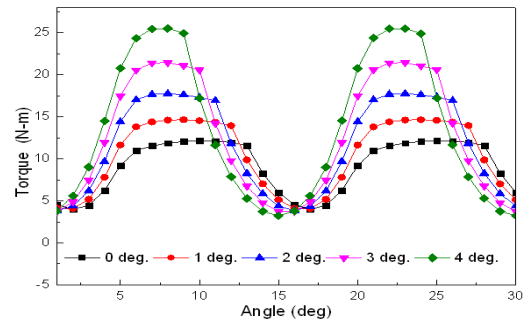


Fig. 5. 12/8 SRM normal excitation angles and orders.



(a) Rotor position for early excitation angle by 3 degrees



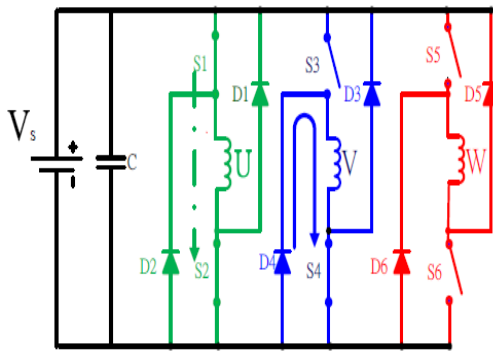
(b) Torque waveforms
Fig. 6. Analysis results

In order to understand the impact of early excitation angle to motor output efficiency in this paper, the different early excitation angles, 1 to 4 degrees respectively, are conducted. And, the the torque waveforms are showed in Fig. 6(b). After analyzing via FEM, the performance parameters, such as the average torque, torque ripple, output power, average current, and efficiency, are recorded in Table 1, where 0 degrees means the normal excitation angle.

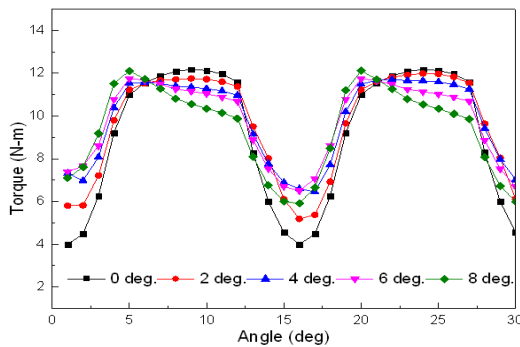
Observing Table 1, as the advanced excitation angle increases, the values of T_{min} and efficiency remain almost the same, while T_{max} , T_{ave} , and T_{Ripple} increase accordingly. Although the output torque increases in accordance with the advanced excitation angle, the current and copper loss also increase, which may cause various problems, e.g., overheating, breaking down on the road, etc. Hence, the advanced excitation angle should be carefully selected for the best motor output efficiency optimization.

Table 1. Output performances of SRM

Angle Performance	0°	1°	2°	3°	4°
T_{Ripple} (%)	67.52	72.21	78.37	82.55	87.32
T_{ave} (N-m)	9.16	10.37	11.58	12.71	13.61
T_{max} (N-m)	11.39	13.49	15.83	18.10	15.13
T_{min} (N-m)	3.99	4.08	4.37	4.87	5.59
Current(A)	60.38	63.61	69.48	78.55	89.09
Power(W)	2301	2605	2909	3193	3419
Efficiecn(%)	86.12	88.72	89.10	88.64	88.34



Delay cut-off time of V-phase button thyristor (S_4)



Torque waveforms
Fig. 7. Analysis results

3.2 Delay the Cut-off Time of Winding Excitation

The control circuit of the SRM driver is shown in Fig. 7(a). Delaying the cut-off time of winding excitation means postponing the end time of the button thyristor (S_4); hence,

energy in the windings is able to be released through diodes, which enables the winding currents to be more continuous. Therefore, in order to investigate the influences of cut-off time on the output torque and torque ripples of the motor, different delayed excitation cut-off angles, such as 2, 4, 6, and 8 degrees, are conducted. And, the the torque waveforms are showed in Fig. 7(b). Through FEM analysis, the performance parameters of average torque, torque ripple, average current, and efficiency are recorded in Table 2.

Shown in Table 2, as the delayed excitation cut-off angle increases, the values of T_{ave} , T_{max} , and efficiency remain almost the same, while T_{min} increases and T_{Ripple} reduces. The torque ripples increase with the delayed excitation angle, which means the delayed excitation cut-off angle should be carefully selected for minimizing torque ripples.

Table 2. Output performances of SRM

Angle Performance	0°	2°	4°	6°	8°
T_{Ripple} (%)	67.18	55.87	44.33	44.71	51.23
T_{ave} (N-m)	9.16	9.63	9.82	9.73	9.32
T_{max} (N-m)	11.39	14.331	14.13	13.77	13.2
T_{min} (N-m)	3.99	5.80	7.32	7.38	7.09
Current(A)	60.38	60.13	58.35	58.75	59.29
Power(W)	2301	2419	2467	2444	2341
Efficiecn(%)	86.12	87.81	87.04	85.65	83.46

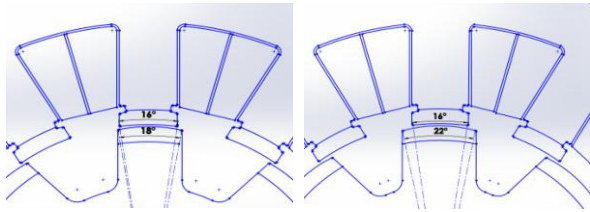
3.3 Adjust the Ratio of Arc Angle between Stator and Rotor

The arc angle ratio strategy attempts to change the ratio of the arc angle between the stator and rotor to understand its influences on motor performance. The original arc angle ratio between the stator and rotor of a 12/8 SRM is 16/18. In this paper, the width of the stator slots is fixed, but the pole arc angle of the rotor is modified. Four different ratios, 16/19, 16/20, 16/21, and 16/22, are examed, as illustrated in Fig. 8(a), and the output performance of the SRM is evaluated. And, the the torque waveforms are showed in Fig. 8(b).

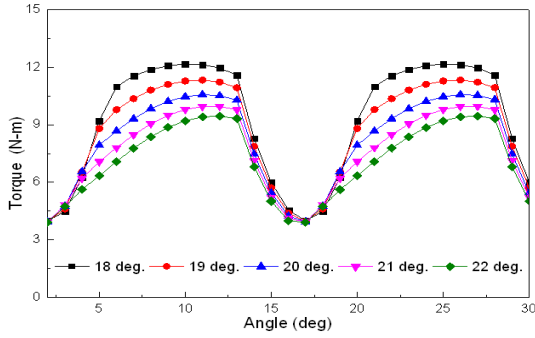
Table 3 shows the values of average output torque, current, power, torque ripple, and efficiency under different arc angle ratios of the reluctance motor.

According to Table 3, although the arc angle of stator increases, T_{min} remains almost the same; T_{max} reduces and thus T_{Ripple} lowers; T_{ave} and efficiency also drop as. Thus, increasing the arc angle ratio may cause output torque of motor to be unable to fulfill the loading requirement. Hence, the arc angle ratio should be selected carefully for optimal motor output performance.

Changing the geometric shape of rotor mainly means that a certain part on each rotor pole tooth is deviated a certain number of degrees, as illustrated in Fig. 9(a), which creates an effect similar to that of skewed rotor; the output performance of such a motor is evaluated.



(i) Arc angle ratio: 16/18. (ii) Arc angle ratio: 16/22.
(a) Ratio of arc angle between stator and rotor.



(b) Torque waveforms
Fig. 8. Analysis results.

Table 3. Output performances of SRM

Ratio Performance	16/18	16/19	16/20	16/21	16/22
$T_{Ripple}(\%)$	67.29	65.14	62.82	60.6	58.68
$T_{ave}(N-m)$	9.16	8.59	8.02	7.53	7.07
$T_{max}(N-m)$	12.18	11.38	10.59	9.92	9.40
$T_{min}(N-m)$	3.99	3.98	3.96	3.93	3.94
Current(A)	60.38	58.3	56.29	54.47	52.86
Power(W)	2301	2158	2015	1892	1776
Efficiency(%)	86.12	87.63	87.13	86.65	86.15

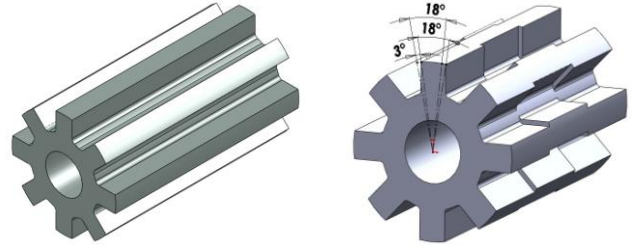
In this paper, 1/3 of each rotor tooth of a 12/8 reluctance motor is deviated 1, 3, 5, and 7 degrees, respectively. The influences of the rotor deviation angle on motor output torque and torque ripples are examined, and the performance parameters of average torque, torque ripple, output power, average current, and efficiency are presented in Fig. 9(b) and Table 4.

In this improved strategy, shown in Table 4, when rotor deviation angle increases, T_{max} increases accordingly, while T_{min} and efficiency remain almost the same; hence, T_{Ripple} and T_{ave} decrease. However, if the deviation angle is too large, the torque tends to increase. Thus, the deviation angle should be evaluated carefully to meet the loading requirement of motor output torque; hence, the motor output performance is optimized.

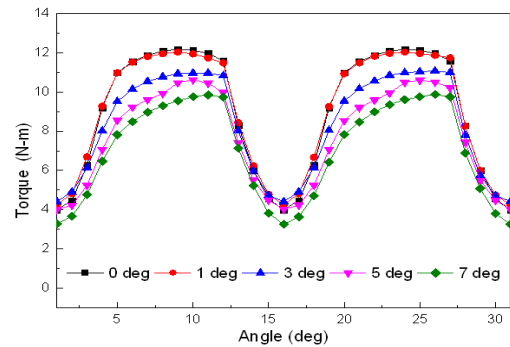
4. Hybrid Design Model for Optimal SRM Design

After the influences of the above mentioned strategies on SRM performance are evaluated, the Taguchi Method is applied to obtain the best combination of the stated strategies to create a hybrid design model, which is adopted

to optimize SRM. The result shows the proposed design model not only reaches the performance target of output torque higher than 8.45N-m and efficiency up to 85%, but also possesses the characteristic of low torque ripple.



(i) Original shape of rotor. (ii) Pole teeth are deviated certain degrees.
(a) 1/3 of rotor tooth is deviated 3 degrees



Torque waveforms
Fig. 9. Analysis results

Table 4. Output performances of SRM

Deviation Performance	0°	1°	3°	5°	7°
$T_{Ripple}(\%)$	67.18	65.0	60.0	62.0	67.0
$T_{ave}(N-m)$	9.16	9.0	8.50	7.82	7.20
$T_{max}(N-m)$	12.18	12.04	10.9	10.45	9.61
$T_{min}(N-m)$	3.99	4.23	4.40	4.00	3.20
Current(A)	60.38	54.46	52.37	50.76	49.7
Power(W)	2301	2261	2135	1964	1809
Efficiency(%)	86.12	86.59	86.98	86.07	86.05

4.1 Quality Objective

The quality objective of this research is to achieve low torque ripple; therefore, the lower-the-better (LB) approach of the Taguchi Method is utilized for analysis, and the signal-to-noise (S/N) ratio is given by

$$S/N = -10\log(MSD) = -10\log\left(\frac{1}{n} \sum_{i=1}^n y_i^2\right) \quad (7)$$

where MSD denotes to the mean square deviation, y_i and n represent the experimental values and experiment times respectively.

4.2 Control Factors and Orthogonal Table

Following the above analysis results, four strategies are defined as control factors A to D; three levels of each control factor are selected, as shown in Table 5, and the L9(3⁴) orthogonal table is plotted to compute the S/N ratio in Table 6.

Table 5. Control factors and levels.

Level Control Factor	1	2	3
A: Early Exciting Angle (deg.)	A1(0)	A2(1)	A3(2)
B: Delayed Cut-off Angle (deg.)	B1(2)	B2(4)	B3(6)
C: Arc Angle Ratio	C1(16/18)	C2(16/19)	C3(16/20)
D: Deviation Angle (deg.)	D1(0)	D2(1)	D3(2)

Table 6. L₉(3⁴) orthogonal table with S/N values

Trial No.	A	B	C	D	S/N
1	A1	B1	C1	D1	5.00
2	A1	B2	C2	D2	6.75
3	A1	B3	C3	D3	9.32
4	A2	B1	C2	D3	5.47
5	A2	B2	C3	D1	6.57
6	A2	B3	C1	D2	9.13
7	A3	B1	C3	D2	5.04
8	A3	B2	C1	D3	5.63
9	A3	B3	C2	D1	7.64

4.3 Response Table and Verification

Table 7. Response table

Level Factor	1	2	3	max.-min.
A	7.0291	7.0615	6.1089	0.9526
B	5.1755	6.3224	8.7017	2.3693
C	6.5925	6.6250	6.9822	0.3896
D	6.4110	6.9793	6.8093	0.5683

According to the S/N values of each trial in Table 6, the S/N response table is gained as Table 7; thus, the optimal parameter combination (A2B3C3D2) is obtained, which induces the lowest number of torque ripples.

In order to understand the contribution of each control factor to quality characteristics, analysis of variance (ANOVA) is employed, and the results are listed in Table 8, in which Factor B (Delayed Cut-off Angle) makes the greatest contribution, and then Factor A (Advanced trigger angle).

Table 8. ANOVA

Index Factor	SS	DO F	Var	F	PC(%)
A	1.75	2	0.8777	24618.2	7.9941
B	19.4	2	9.7055	272231.3	88.4002
C	0.28	2	0.1402	3933.2	1.2772
D	0.51	2	0.2552	7159.7	2.3249
e	0.00	2	-	-	-
e _T	0.00	(2)	4e-05	10.9787	0.0036
T	21.9	10	-	-	-

4.4 Hybrid Design Model

The optimal parameter combination (A2B3C3D2) is obtained with the application of the Taguchi Method, with which the SRM is optimized by advancing the excitation angle for 1 degrees (A2), delaying low-side excitation cut-off angle for 6 degrees (B3), setting arc angle ratio between the stator and rotor to be 16/20 (C3), and utilizing 1 degree of rotor deviation (D2).

After FEM analysis, under the rotation speed of 2400rpm, the magnetic flux distribution and running torque are illustrated in Figures 10 and 11, respectively. The comparison of the motor performances before and after optimization is made and is presented in Table 9.

4.5 Implementation and Experimentation

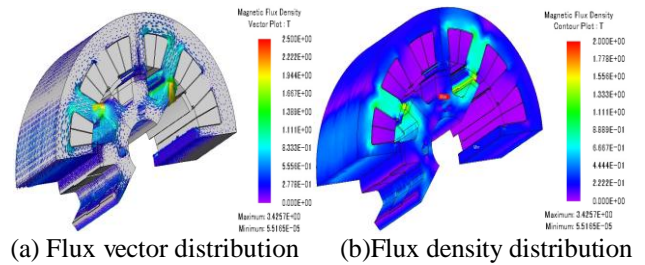


Fig. 10. FEM analysis (1/2 cross-sectional view)

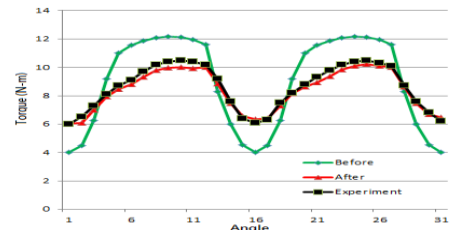


Fig. 11. Waveforms of running torque before/after optimization

Table 9. Motor performances before/after optimization

Optimization Performance	Before	After	Experiment
T _{Ripple} (%)	67.18	37.19	40.00
T _{ave} (N-m)	9.16	8.45	8.61
T _{max} (N-m)	12.18	10.02	10.60
T _{min} (N-m)	3.99	6.41	6.30
Current(A)	60.4	53.59	54.29
Efficiency(%)	86.1	87.1	86.8



(a) Stator (b) Rotor
Fig. 12. Prototype of proposed SRM



Fig. 13 Experimental Platform

From Fig. 11 and Table 9, via the proposed hybrid design model, the SRM not only reaches the target of 8.45N-m running torque and efficiency up to 87.1%, but also reduces significantly the torque ripples by 30%, from 67.2% to 37.2%.

Fig. 12 shows the prototype of the proposed SRM. Figure 13 shows the SRM experimental platform. The experimental results are summarized in Table 9. Both the running torque and the efficiency are 8.61 N-m and 86.8%, respectively. In addition, the torque ripple is 40.0% close to the design value of 37.19%. Thus, the performance of the SRM prototype also reaches the design targets. The achievement verifies that the hybrid design strategy model consisting of the optimal parameter combination computed by the Taguchi Method is capable of fulfilling the purpose of reducing SRM torque ripples and enhancing output torque and efficiency.

5. Discussion and Conclusion

In order to effectively reduce torque ripples, four design strategies are commonly used, which are (i) changing the excitation trigger angle of stator windings, (ii) delaying the cut-off time of winding excitation, (iii) adjusting the ratio of arc angle between stator and rotor, and (iv) changing the geometric shape of rotor. However, when these strategies are solely applied to reduce the torque ripples of the SRM, then the output torque and efficiency may drop accordingly.

According to the analysis results of this study, it shows the following:

Though the early excitation strategy has a small impact on efficiency but helps to improve torque; however, torque ripples will greatly increase;

Delaying the cut-off time to the button thyristor can limit effect of torque ripple, but the efficiency is also decreased;

The smaller the arc angle ratio between the stator and rotor is, i.e., the arc angle of the rotor becomes bigger, the slightly lower the output torque, torque ripple, and efficiency are;

The larger the deviation angle of the rotor is, the lower the torque ripple and the efficiency are. However, if the

deviation angle is too significant, on the contrary, torque ripples increase.

Referring to the analysis above, each strategy has both its advantages and disadvantages. In this paper, the Taguchi Method is applied to determine the best parameter combination from the four stated strategies to form a hybrid design strategy model to optimize SRMs. The experimental results show that the proposed hybrid design model not only can reach high motor output torque but also greatly reduces torque ripples by 27.18%. The research results are expected to contribute to related investigations and production and assist in enhancing the manufacturers' techniques in developing high performance switched reluctance motors.

Acknowledgement

The authors gratefully acknowledge financial supports from the National Science Council of R.O.C. under contract NSC 101-2221-E-244-011 and the Ministry of Economic Affairs of R.O.C. under contract MOEA 100-EC-17-A-05-S1-192.

References

- [1] K. M. Rahman and S. E. Schulz, "Design of high-efficiency and high-torque-density switched reluctance motor for vehicle propulsion," *IEEE Trans. Ind. Appl.*, Vol. 38, No. 6, Nov./Dec. 2002, pp. 1500-1507.
- [2] S. Wang, Q. Zhan, Z. Ma, and L. Zhou, "Implementation of a 50-kW four-phase switched reluctance motor drive system for hybrid electric vehicle," *IEEE Trans. Magn.*, Vol. 41, No. 1, pp. 501-504, Jan 2005.
- [3] H. Hayashi, K. Nakamura, A. Chiba, T. Fukao, K. Tungpimolrut, and D. G. Dorrel, "Efficiency improvements of switched reluctance motors with high-quality iron steel and enhanced conductor slot fill," *IEEE Trans. Energy Convers.*, Vol. 24, No. 4, pp. 819-825, Dec. 2009
- [4] M. Takeno, A. Chiba, N. Hoshi, S. Ogasawara, M. Takemoto, and M. A. Rahman, "Test results and torque improvement of the 50-kW switched reluctance motor designed for hybrid electric vehicles," *IEEE Trans. Ind. Appl.*, Vol. 48, No. 4, pp. 1327-1334, July/Aug. 2012.
- [5] T. Suzuki, S. Ito, N. Tanaka, A. Chiba, T. Fukao, and H. Ninomiya, "Development of high efficiency of switched reluctance motor," *Inst. Electr. Eng. Jpn., Papers Tech. Meeting Rotating Mach.*, vol. 126, no. 4, pp. 511-518, 2006.
- [6] Y. Hasegawa, K. Nakamura, and O. Ichinokura, "Optimization of a switched reluctance motor made of permendur," *IEEE Trans. Magn.*, Vol. 46, No. 6, pp. 1311-1314, June 2010.
- [7] F. Sahin, H. B. Ertan, and K. Leblebicioglu, "Optimum geometry for torque ripple minimization of switched reluctance motors," *IEEE Trans. Energy Convers.*, vol. 15, no. 1, Mach 2000.
- [8] W. Cai and P. Pillay, "Resonant frequencies and mode shapes of switch reluctance motors," *IEEE Trans. Energy Convers.*, vol. 16, no. 1, pp. 43-48, March 2001.

- [9] T. Boukhobza, M. Gabsi, and B. Grioni, "Random variation of control angles, reduction of SRM vibrations," IEEE International Electric Machines and Drives Conference, pp. 640-643, 2001.
- [10] A. E. Fitzgerald, C. Kingsley, Jr., and S. D. Umans, *Electric Machinery*, McGraw-Hill, 2002.
- [11] M. C. Costa, S. I. Nabeta, A. B. Dietrich, J. R. Cardoso, Y. Marechal and J. L. Coulomb, "Optimisation of a switched reluctance motor using experimental design method and diffuse elements response surface," IEE Proc.-Sci. Meas. Technol., Vol. 151, No. 6, pp.411-413, Nov. 2004.
- [12] N. K. Sheth and K. R. Rajagopal, "Optimum pole arcs for a switched reluctance motor for higher torque with reduced ripple," IEEE Trans. Magn., Vol. 39, No. 5, pp. 3214-3217, Sept. 2003.
- [13] B. Mirzaeian, M. Moallem, V. Tahani, and C. Lucas, "Multiobjective optimization method based on a genetic algorithm for switched reluctance motor design, IEEE Trans. Magn., Vol. 38, No. 3, pp. 1524-1527, May 2002.
- [14] Y. K. Choi, H. S. Yoon, and C. S. Koh, "Pole-shape optimization of a switched-reluctance motor for torque ripple reduction," IEEE Trans. Magn., Vol. 43, No. 4, pp. 1797-1800, April 2007.
- [15] N. K. Sheth and K. R. Rajagopal, "Torque profiles of a switched reluctance motor having special pole face shapes and asymmetric stator poles," IEEE Trans. Magn., vol. 40, no. 4, pp. 2035-2037, Jul. 2004.
- [16] J. W. Lee, H. S. Kim, B. I. Kwon, and B. T. Kim, "New rotor shape design for minimum torque ripple of SRM using FEM," IEEE Trans. Magn, vol. 40, no. 2, pp. 754-757, Mar. 2004.
- [17] Y. Murai, C. Ji, S. Sugimoto and M. Yoshida, "A capacitor-booster, soft switched switched-reluctance motor drive," in Proc. IEEE Applied power Electronics Conference and Exposition, vol. 1, pp. 424-429, 1999.
- [18] T. J. E. Miller, *Switched Reluctance Motor and Their Control*, Oxford Press, New York, 1993.
- [19] S. I. Kim, J. Y. Lee, Y. K. Kim, J. P. Hong, Y. Hur, and Y. H. Jung, "Optimization for reduction of torque ripple in interior permanent magnet motor by using the Taguchi Method," IEEE Trans. Magn., Vol.41, No.5, pp.1796-1799, May 2005.



Zwe-Lee Gaing received the Ph.D. degree from National Sun Yat-Sen University in Taiwan in 1996. From 1997 to 2004, he worked as an Assistant Professor with the Electrical Engineering Department of Kao-Yuan Institute of Technology, Kaohsiung County, Taiwan. Since 2005, he has been a Professor with the Electrical Engineering Department, Kao-Yuan University, Kaohsiung City, Taiwan. His research interests include the applications of artificial intelligence techniques, the optimal operation of power system, motor design and control for electric vehicle. (e-mail: zlgain@cc.kyu.edu.tw).



Yao-Yang Hsieh was born in Kaohsiung City, in 1989. He received the M.S. degree in electrical engineering from Kao-Yuan University, Kaohsiung City, Taiwan in 2013. His research interests include the applications of artificial intelligence techniques, traction motor design for electric vehicle. (e-mail: forever770921@yahoo.com.tw).



Mi-Ching Tsai received the B.S. and M.S. degrees in Electronic Engineering from National Taiwan University of Science and Technology, Taiwan, in 1981 and 1983, respectively, and the Ph.D. degree from the Department of Engineering Science, University of Oxford, U.K., in 1990. He is currently a Chair Professor at the Department of Mechanical Engineering and the Director General of Research & Services Headquarter, National Cheng Kung University, Taiwan. His research interests include servo control, motor design, and mechatronics. (e-mail: mct sai@mail.ncku.edu.tw)



Min-Fu Hsieh was born in Tainan, Taiwan. He received the B.Eng. degree in mechanical engineering from National Cheng Kung University (NCKU), Tainan, in 1991 and the M.Sc. and Ph.D. degrees in mechanical engineering from the University of Liverpool, Liverpool, U.K., in 1996 and 2000, respectively. Since 2012, he has been a Full Professor with the Department of Systems and Naval Mechatronic Engineering, NCKU, where he was a Researcher with the Electric Motor Technology Research Center from 2000 to 2003. In 2003 he was appointed as an Assistant Professor and later promoted to Associate Professor. His areas of interests include renewable energy generation (wave, tidal current, and wind), electric machine design, and servo control. Prof. Hsieh is a member of the IEEE Industry Applications, IEEE Magnetics, and IEEE Industrial Electronics Societies. (e-mail: forever770921@yahoo.com.tw)



Ming-Hsiao Tsai was born in Chayi County, Taiwan. He received the B.S. and M.S. degrees from Department of Electrical Engineering of Kao Yuan University, Taiwan, in 2008 and 2010, respectively. His research interests include high-effective motor/generator design and special electric vehicle design. Since 2012, He has been as a research assistant in EMTRC of National Cheng Kung University. He main task is to design a high-effective switched reluctance motor for electric vehicles. (e-mail: minghsiao2005@gmail.com)